Published in final edited form as:
Neuromuscul Disord. 2012 October 1; 22(Suppl 2): S111–S121. doi:10.1016/j.nmd.2012.05.013.

MRI/MRS Evaluation of a Female Carrier of Duchenne Muscular Dystrophy

Sean C. Forbes, PhD[1], **Donovan J. Lott, PT, PhD**[1], **Richard S. Finkel, MD**[2], **Claudia Senesac, PT, PhD**[1], **Barry J. Byrne, MD**[3], **H. L. Sweeney, PhD**[4], **Glenn A. Walter, PhD**[5], and **Krista Vandenborne, PT, PhD**[1]

[1]Department of Physical Therapy, University of Florida, Gainesville, Florida

[2]The Children's Hospital of Philadelphia, Philadelphia, Pennsylvania

[3]Departments of Pediatrics and Molecular Genetics & Microbiology, Powell Gene Therapy Center, University of Florida, Gainesville, Florida

[4]Department of Physiology, University of Pennsylvania, Philadelphia, Pennsylvania

[5]Department of Physiology and Functional Genomics, University of Florida, Gainesville, Florida

Abstract

The purpose of this study was to evaluate skeletal muscle composition of lower extremity muscles in a manifesting female carrier of Duchenne muscular dystrophy (MFC_{DMD}) using magnetic resonance imaging (MRI) and spectroscopy (MRS). MRI/MRS was performed on the lower extremities and heart of a MFC_{DMD} (47yr, 51kg) on four occasions within 21 months and in a control subject. Heterogeneity and asymmetry among muscles in the MFC_{DMD} was observed in lipid fraction and mean transverse relaxation time (T_2) of lower extremity muscles with some muscles presenting as unaffected (e.g., rectus femoris) and others showing substantial deterioration and lipid infiltration (e.g., vasti muscles). There was an association of abnormal MRI findings and strength and motor function. Over the 21 months a small decrease in CSA_{max} and increase in lipid fraction and T_2 was observed in the MFC_{DMD} in some muscles. In summary, this MFC_{DMD} revealed significant imaging evidence of pathologic heterogeneity among muscles. Furthermore, this study shows the feasibility of combining various quantitative MRI and MRS approaches to monitor skeletal muscle involvement.

Keywords

female carrier; Duchenne muscular dystrophy; magnetic resonance imaging; magnetic resonance spectroscopy; skeletal muscle; biomarker

Introduction

Duchenne muscular dystrophy (DMD) is a genetic disease that is caused by mutations in the dystrophin gene [1]. DMD has a prevalence of 1 in 3,600–6,000 male births, and is characterized by progressive muscle weakness, deteriorating functional capabilities, loss of

Corresponding Author: Krista Vandenborne, PT, PhD, Department of Physical Therapy, Box 100154, UFHSC, Gainesville, FL 32610.

independence, and early death [2]. Although DMD is an X-linked recessive disease, it is not uncommon for female carriers of DMD to report symptoms, including muscle pain [3], cramping [4], weakness [4] and cardiac dysfunction [5,6]. Hoogerwaard et al. (1999) reported 22% of female carriers manifested symptoms, with 19% demonstrating muscle weakness measured by handgrip strength and manual muscle testing and 8% presenting with dilated cardiomyopathy. A similar prevalence of females with symptoms was observed by Grain et al. (2001), with 12% presenting with muscle weakness and 7% displaying cardiomyopathies. Onset of symptoms typically occur in early adulthood but in some cases have been reported in children [7,8]. Muscle weakness of the proximal muscles, such as the shoulder and pelvic girdle musculature, is common and usually presents in an asymmetrical manner [4]. The specific muscles affected are variable [4], with a range of severity from no muscle weakness to being wheelchair bound [7].

The signs and symptoms of a manifesting female carrier of Duchenne muscular dystrophy (MFC_{DMD}) have been suggested to be due to X-autosomal translocations leading to skewed X-inactivation of the normal dystrophin gene [9]. Alternatively, there may be impaired production of the dystrophin protein due to other, still unknown, genetic factors altering the protein levels [10]. A mosaic pattern of dystrophin-positive and dystrophin-negative fibers has previously been reported in MFC_{DMD} [11], and elevated levels of creatine kinase are commonly observed [12].

Overall, skeletal muscle involvement in MFC_{DMD} appears to be variable among individuals and muscles. Previous studies have mainly utilized self-reports [13], manual muscle testing [14], hand-held dynamometry strength tests [4], and muscle biopsies of single muscles [15]. Also, magnetic resonance imaging (MRI) has been used to provide a qualitative assessment of thigh muscles [16] and to examine proton spin lattice relaxation time (T_1) in female carriers at a low magnetic field strength [17]. In that study T_1 was elevated in the gluteals, vastus lateralis (VL), and gastrocnemius of MFC_{DMD} relative to controls, and this was attributed to an increase in edema [17]. However, in general, the use of MR to evaluate skeletal muscles of MFC_{DMD} has been limited.

A more comprehensive assessment of numerous muscles in the legs and thighs of MFC_{DMD} could provide additional insight regarding this population. Therefore, the purpose of this study was to evaluate a MFC_{DMD} using MRI and magnetic resonance spectroscopy (MRS) to examine structure and composition of multiple muscle groups of the lower extremities, as related to functional abilities and bilateral lower extremity strength, and to follow progression of lower extremity MRI measures over 21 months.

Methods

A MFC_{DMD} (47yr, 51 kg, 161.5 cm) who reported symptoms of muscular weakness and a female control subject (Con) of similar age and body size (45 yr, 50 kg, 158.0 cm) volunteered to participate in this study. The Con was not involved in any sport specific training. The study was approved by the University of Florida Institutional Review Board and an informed written consent was obtained from the subjects prior to participation in the study.

Subject history

The MFC_{DMD} reported that she first noticed lower extremity weakness approximately 10 years prior to the initial time point, and that at first the weakness was most prominent in the right thigh/quads region. She was able to perform recreational activities, such as skiing, into her 30s. She reported that her left anterior leg muscles were increasingly becoming weak, and shortly prior to her final testing session received a prescription for an ankle foot orthosis

to address foot drop, which became more evident with fatigue. Her medications included deflazacort (6mg/day) and calcium supplements (500 mg/day) during the study. Her son has typical features of DMD; both have the same dystrophin mutation caused by a premature termination codon at exon 61 (c.9100C>T; p.Arg3034X).

Longitudinal MRI/MRS measures were acquired on the lower extremity muscles at three time points over 21 months and in the heart on one occasion. The right lower extremity was studied at baseline (T0), 9 months (T9), and at 21 months (T21). The cardiac scan was performed at 13 months (T13) and the left lower extremity was scanned at T21. Strength testing of the lower extremities and functional testing was also performed at T21. MRI and MRS were performed on the right lower extremity of the Con at one time point.

MR Data Acquisition

MR scans were performed using a 3T Philips Achieva system (Philips Medical Systems, R2.6.3). Initially, the subjects were placed supine in the bore of the magnet with the leg secured using foam padding and weighted rice bags. An 8-channel SENSE volume knee coil (Invivo corp.) was used for the lower leg and a 2-channel FLEX surface coil (Invivo corp.) was used for the thigh.

Lower extremity skeletal muscles were evaluated using T_1-weighted 3-D gradient echo (GE) images with spectral presaturation by inversion recovery (SPIR) fat suppression (lower leg: FOV 120×120×146 mm, TR 17 ms, TE 1.9ms, and 20° flip angle; upper leg: FOV 170×170×146 mm, TR 24 ms, TE 1.8 ms, 20° flip angle) and without fat suppression (lower leg: FOV 120×120×146 mm^3, TR 4.9 ms, TE 1.9ms, and 20° flip angle; upper leg: FOV 170×170×146 mm^3, TR 6.1 ms, TE 1.4 ms, and 20° flip angle). Three-point (3Pt) Dixon images were acquired on both the lower leg and thigh (25 axial slices, TR 430 ms, 20° flip angle) and T_2-weighted SE images (18 axial slices, TR 3 s, 5 TE's: 20–100 ms) were acquired on the lower leg. Also, a ^{1}H-MRS scan was performed at each time point to test the feasibility of these measures; these measures were not intended to provide longitudinal comparisons. Specifically, single voxel ^{1}H-MRS (TR 9s; 16 echoes: 10, 14, 18, 27, 36, 45, 54, 63, 90, 81, 90, 108, 135, 162, 198, 243, and 288 ms) was acquired using STEAM from the right medial gastrocnemius (MG) at the first time point and the right soleus (Sol) at the second time point. Multi-voxel spectroscopy was performed using 2D PRESS chemical shift imaging (TR 2s, TE 108 ms, FOV 12×12 cm; 12×12 matrix) in an axial slice of the lower left leg at the third time point. Finally, cardiac images were acquired using ECG-gated Turbo Field Echo CINE (15 short axis slices, 25 frames/cardiac cycle, TR 5.9 ms, TE 3.6 ms) with a 16-channel torso array coil (Philips Healthcare) without any contrast enhancement.

MR Analysis

CSA_{max}—Maximal cross sectional area (CSA_{max}) was measured for the tibialis anterior (TA), extensor digitorum longus (EDL), peroneus longus and brevis (Per), Sol, lateral gastrocnemius (LG), MG, tibialis posterior (TP), rectus femoris (RF), semitendinosis, (ST), vastus lateralis (VL), gracilis (Gra), and sartorius (Sar) (Figure 1). The muscles were manually traced using the fat suppressed and non-suppressed GE images in OsiriX software (v3.8.1; http://www.osirix-viewer.com). The CSA_{max} was defined as the average of the largest CSA of a muscle in an axial slice and the CSA in the adjacent proximal and distal slices, resulting in an average of three slices.

Lipid fraction—Three-point Dixon axial lipid and water maps of the lower extremity were reconstructed using Philips software (R2.6.3) and custom written software using Interactive Data Language (IDL; Excelis Visual Information Solutions, Inc.) and Matlab (Mathworks,

Inc.). Axial slices of the lower leg and thigh that had a large representation of each of the muscles of interest were chosen (Figure 2). Specifically, the most proximal slice that the flexor digitorum longus (FDL) was evident was utilized as well as the adjacent proximal and distal slice to produce a weighted-average of three contiguous slices. For the thigh, the most proximal axial slice that the biceps femoris-short head (BFs) was visually evident was utilized, as well as the adjacent proximal and distal slice. Seven muscles of the lower leg [TA, EDL, Per, Sol, LG, MG, and TP] and 11 muscles of the thigh [RF, VL, vastus intermedius (VI), vastus medialis (VM), biceps femoris-long head (BFl), ST, semimembranosus (SM), adductor longus (AL), adductor magnus (AM), Gra, and Sar] were evaluated. Regions of interests (ROI) for muscles were created using the reconstructed water and lipid images with care to avoid the fascia between muscles. This ROI was then utilized to calculate lipid fraction [i.e., lipid signal/(water+lipid signal)] and a saturation correction factor was applied for using lipid T_1 of 459 ms [18] and water T_1 of 1.35 s. T_1 of water was estimated using the ^1H_2O signal from the ^1H spectroscopy acquisition (TE 108 ms) at 3 and 9 s TR in the MG of the female carrier, which was similar to the literature values of control subjects [19].

T_2 mapping—T_2 values were calculated for lower leg muscles by creating T_2 maps using echo numbers 2–5 with a mono-exponential equation. Excluding the first TE has previously been shown to reduce error in the T_2 measurement due to minimizing the effect of stimulated echoes, and therefore was omitted for this analysis [20]. Pixel-by-pixel T_2 maps were generated using OsiriX software (v3.8.1; http://www.osirix-viewer.com) in three consecutive slices corresponding to the largest cross sectional area of the lower leg with the center slice being in the region in which the most proximal slice the FDL was visually present, as described above. Therefore, the mean T_2 was the average of all the pixels in the muscle of the three slices. The regions of interest were carefully drawn within the borders of the muscle to avoid any potential contamination of inter-muscular fascia.

Spectroscopy measures of muscle composition—The spectroscopic T_2 values were derived using the amplitude of the ^1H_2O signal at non-linear spaced TE's using principal component analysis [21], then the kinetics subsequently resolved using a mono-exponential model and non negative least squares (NNLS) analyses (500 time constants linearly spaced from 2 to 200 ms, plus an energy constraint) [22]. The relative contribution of each component to the overall response was determined by the area under the curve. Also, multi-voxel spectroscopy was utilized to provide an estimate of relative lipid concentration of the lower leg muscles. ^1H CSI data were analyzed using 3DiCSI software (Version 1.9.7) [23], in which spectra were zero-filled to 24×24, phased and summed to produce a single spectrum for each muscle group.

Cardiac MR—CAAS MRV software (Pie Medical Imaging) was used to calculate myocardial ejection fraction. The epicardium and endocardium were manually traced in the end-diastolic and end systolic frame of each slice from the base to the apex of the heart with inclusion of the papillary muscles. Borders were manually traced at end-diastole, which was the first image in the ECG-gated cardiac set and end-systole, defined as the frame with the minimal cross sectional area.

Function and Strength

Isometric peak torque of the knee extensors of each leg was measured using a Biodex dynamometer as has previously been described [24]. For strength testing, the knee and hip joints were placed at 90° of flexion. The subject was instructed to push maximally for 5 seconds, followed by 1-minute of rest. At least five trials were performed for each leg, and the highest torque value was designated as peak torque.

The MFC_{DMD} performed three functional tasks: 1) time to walk/run 10m; 2) time to ascend 4 steps; and 3) the 6-min walk test. The subject was given rest breaks between tasks to minimize the effects of fatigue, and heart rate and blood pressure were monitored before and after the 6-min walk test. The subject performed the 10 m walk/run and stairs three times each, and the fastest time was used for analysis. During the tasks, qualitative descriptions of performance were noted by a trained Physical Therapist. Also, the functional ability of the MFC_{DMD} was ranked using the Modified Brooke Lower Extremity Scale [25]. This scale ranges from grade 1 (able to walk and climb stairs independently) to grade 10 (confined to bed).

Results

The MFC_{DMD} participated in this study at four time points over 21 months, during which time she maintained a similar body mass at each visit (50–51 kg) and remained fully functional in performing her regular daily activities. Her ejection fraction was 50%, and therefore she did not appear to have severe clinical cardiomyopathy.

Cross-sectional area of lower extremity muscles

Maximum cross-sectional area (CSA_{max}) was measured in muscles of the lower leg and thigh (Figure 1). Maximal girth (circumference) of the thigh was 39% less and the calf was 13% greater in MFC_{DMD} than Con. However, there was considerable variation among individual muscles (Table 1; Figure 3), with some muscles being smaller in the MFC_{DMD} than Con [e.g., RF, TA (left), EDL (right), VL (right), and Gra], while other muscles were larger in the MFC_{DMD} than Con (e.g., LG, ST, and Sar).

Distinct differences were observed between the left and right lower extremity muscles in the MFC_{DMD}, with several muscles showing > 20% difference in size between legs, including the TA, LG, EDL, TP, ST, and Gra (Table 1). Notably, the CSA_{max} of the Gra was more than two-fold greater in the left than the right thigh. In the right lower extremity, longitudinal measures were acquired over 21 months, and, on average, there was a small decrease in muscle size over this time (mean reduction of 5±7%) with the Sol and Gra showing the greatest relative decrease of the muscles examined (Table 1).

Muscle Composition

Quantitative MRI measures were acquired to evaluate muscle composition in the MFC_{DMD}, including 3pt Dixon (Figure 2) and T_2 mapping. Three-point Dixon was utilized to estimate lipid fraction, and these measures were relatively homogenous among the muscles examined in Con, ranging between 5–6% in the lower leg and 8–14% in the thigh muscles (Figures 4 and 5). In contrast, in the MFC_{DMD} there was considerable heterogeneity among lipid fraction measures ranging from 8–71% in the lower leg and 8–67% in the thigh (Figures 4 and 5). Among the lower leg muscles, the MG and anterior compartment muscles had the most lipid infiltration, whereas the LG and TP appeared to be relatively preserved (Figure 4a). The substantial lipid infiltration in the MG was also revealed when observing the lipid/water ratio using CSI ^1H spectroscopy (Figure 6). In the quadriceps femoris, the vasti muscles had considerable fatty tissue infiltration (>40%), whereas the RF (11%) had the lowest values (Figure 5a). Among the hamstring muscles, the BFl was most infiltrated with lipid (62%), while the ST had the least amount of lipid among these muscles (10%) (Figure 5a). The adductors also had a range of lipid values among muscles with the AM having the highest lipid fraction (38%) and the Gra the lowest (11%) (Figure 5a).

There were also several notable differences between lower legs in the same muscles. For example, the TA and MG had ~ 2 fold greater lipid infiltration in the left than the right leg,

while the EDL had considerably greater lipid levels in the right (56%) than the left (16%) (Figure 4a). In the thigh, there was also asymmetry in lipid infiltration of muscles, such as the AM having greater lipid in the right (48%) than the left (28%) leg (Figure 5a). The longitudinal measures acquired over 21 months in the right lower extremity showed, on average, a 3% increase in the lipid fraction in the lower leg muscles (Figure 4b) and a 5% increase in relative lipid fraction in the thigh muscles (Figure 5b). The relative lipid concentration progressed fastest in the MG of the lower leg (13% increase) and most rapidly in the VI of the thigh muscles (11% increase) over the 21 month time period.

MRI-T_2 was measured in the lower leg in the MFC_{DMD} and in the Con. T_2 values were more homogenous among muscles in Con, ranging from 34.0 ms (TA) to 40.7 ms (Per), compared to MFC_{DMD} in which T_2 values ranged from 47.3 ms (Sol) to 81.0 ms (EDL) (Figure 4c). As in the lipid measures, T_2 also showed asymmetry between muscles in the left and right legs. For example, the TA was elevated in the left leg (77 ms) compared to the right leg (53 ms), while the EDL was lower in the left (49 ms) compared to the right (81 ms). Overall, there was a small increase in T_2 over 21 months in the leg muscles (2.2ms), with the MG and EDL showing the most rapid progression (Figure 4d). T_2 was also measured using ^{1}H-MRS in the MG and Sol. T_2 of $^1H_20$ was greater in the MG (32.4 ms) and Sol (30.4 ms) of the MFC_{DMD} than in the Sol of Con (28.5 ms) (Figure 7). Furthermore, when NNLS was performed there was a long component evident in the MG (T_2: 76 ms; Amplitude: 3%) and Sol (T_2: 121 ms; Amplitude: 1%) of the MFC_{DMD} but not in Con (Figure 6).

Function and Strength

The MFC_{DMD} was able to complete the leg extension strength assessment, stair climbing, 10 m walk/run and 6 minute walk test. The subject demonstrated 21% greater strength with her left than right leg during leg extension (Table 2). She ascended the four steps by alternating feet on the steps and required the assistance of her arms using both handrails. While descending the steps she was observed to alternate feet while using the handrails for support. While walking at a self-selected pace on a level surface for the 6 minute walk test the subject exhibited the following gait deviations: 1) high steppage gait pattern with excessive and pronounced hip and knee flexion during early to mid swing phase for both lower extremities; 2) decreased dorsiflexion bilaterally as evidenced by a foot drop during mid to late swing phase, which was more pronounced with the left foot; 3) genu recurvatum during mid to late stance phase that was more evident on the left than right; and 4) positive Trendelenburg noted during both the right and left stance phase of gait. Both the foot drop and genu recurvatum (left greater than right) became more pronounced as the subject continued with the 6 minute walk test, which appeared to be related to fatigue.

Discussion

This is the first study to provide a comprehensive evaluation of lower extremity muscles in a symptomatic female carrier of DMD using MRI and MRS. The main findings of this study were: 1) considerable heterogeneity among lower extremity muscles of the MFC_{DMD}, ranging from some muscles displaying properties of severe involvement and deterioration (MG, AM, BFl, VL, VI, and VM) and other muscles appearing relatively preserved (TP, RF, ST, and Gra); 2) bilateral leg asymmetry in several muscles, evident by differences in CSA_{max}, lipid infiltration, and T_2; 3) progressive increase in lipid infiltration and T_2 of some lower extremity muscles over 21 months (MG, VI, VM, SAR, and RF), while several other muscles maintained similar values over this time; and 4) alterations in muscle composition were associated with decrements in functional performance and strength. Collectively, the results suggest that MR is valuable in detecting affected muscles and following disease progression and may be used to follow possible treatments in female carriers of DMD.

Using MRI/MRS to evaluate skeletal muscles of female Carrier of DMD

Female carriers of DMD have a range of severities of being affected. While the majority of carriers appear to be asymptomatic, there are a significant number of carriers that have been observed to manifest symptoms resulting in skeletal muscle weakness [4,14]. In lower extremity skeletal muscles of the female carrier observed in this study there was evidence of increased lipid infiltration and elevated T_2 values compared to a control subject of similar age and body mass. Lipid fraction was estimated using three-point Dixon imaging, which exploits the chemical shift difference in water and lipid to produce high resolution water and lipid images. The three-point method has the advantage of minimizing the effects of field inhomogeneity [26], and has been utilized in previous studies to examine skeletal muscle involvement in DMD [27] and other dystrophies [28]. MRI T_2 reflects a number of physiological factors, including fatty tissue infiltration [29], fibrosis [30], and muscle damage [31]. The elevated MRI T_2 values in the female carrier observed in this study were likely primarily reflective of the elevated lipid levels in the muscles. In support of this notion, MRI-T_2 was strongly associated with the lipid fraction measures (r=0.87). However, when T_2 of $^1H_20$ was measured independent of lipid using ^{1}H-MRS in the Sol and MG, an elevated T_2 was observed in the MFC_{DMD} compared to Con, suggesting that factors related to muscle damage and inflammation/edema independent of fatty tissue replacement also contributed to the elevated T_2 in the MFC_{DMD}. This elevation in T_2 in the MFC_{DMD} may be analogous to the increase in T_2 observed following eccentric-induced muscle damage in humans [31], in dystrophic mice [32], and exercised rats [33]. Furthermore, when NNLS analysis was performed there was a long component evident in the MG and Sol of MFC_{DMD} but not in the control subject, consistent with an edema-like fluid accumulation in the female carrier. A long component has previously been observed in skeletal muscle using NNLS when edema was induced using lower body negative pressure in the lower leg [34]. Therefore, the measures of lipid infiltration and T_2 revealed dramatic differences between Con and the MFC_{DMD}.

Over 21 months, on average, a small decrease in CSA_{max} and increase in lipid fraction and T_2 was observed in the MFC_{DMD}. While some muscles seemed to worsen (MG, VI, VM, SAR, and RF), several other muscles appeared to remain stable. A more comprehensive evaluation of the sensitivity of these MR measures to detect changes in female carriers over time will require further investigation with a larger sample size, and future studies may also benefit from measures throughout the length of the muscles including both proximal and distal regions.

Heterogeneity of Structure and Composition of Lower Extremity Muscles

A range of preserved to severely affected muscles were observed in the lower extremity muscles of the MFC_{DMD}. Different levels of involvement were observed within each functional muscle compartment. For example, in the quadriceps femoris the RF was relatively preserved, whereas the VL, VM, and VI were diminished in size with a large fraction of lipid compared to Con. Of the hip adductor muscles, the Gra and Sar were less affected, whereas the AM showed significant involvement. Of the hamstring muscles, the ST was relatively preserved, whereas the SM and BFl were considerably more affected. Therefore, each of the functional and regional muscle compartments of the thigh had a range of involvement among the individual muscles. Furthermore, several of the muscles examined were affected to a different extent between the left and right lower extremities. For example, the EDL had greater lipid fraction and elevated T_2 in the right than the left leg, whereas the TA was considerably more affected in the left than the right leg. This bilateral asymmetry is consistent with previous reports using manual muscle testing of female carriers of DMD [8].

The pattern of involvement of affected muscles in the female carrier appears similar to children with DMD in some ways, but clearly different in other respects. For example, both the MFC_{DMD} and children with DMD tend to have enlarged plantar flexor calf muscles [15,24]. Also, the TP, Gra, and Sar seem to be relatively preserved in DMD [35] and were relatively preserved in the female carrier observed in this study. On the other hand, the RF appeared to be the most affected of the quadriceps femoris muscle group in boys with DMD [36], whereas in this MFC_{DMD} the RF was the most preserved quadriceps femoris muscle. These seemingly unsystematic affected muscles in female carriers are consistent with the view that random X-autosomal translocations leads to skewed X-inactivation of the normal dystrophin gene in muscles [9]. Therefore, presumably the affected muscles observed in this study reflect muscles that lack functional dystrophin.

Several of the muscles that were relatively unaffected in the MFC_{DMD} appeared to have undergone a compensatory hypertrophic response. For example, the cross sectional area of the ST was considerably greater in the MFC_{DMD} than Con (despite having similar lipid fraction), possibly to compensate for the diminished muscle in other hamstring muscles, such as BFl. Similarly, in the left MG of the female carrier the muscle content appeared to be several fold less compared to Con (estimated by water fraction from 3pt dixon*CSAmax). This small amount of contractile tissue may have resulted in a compensatory increase in muscle size in the LG, which was over two-fold greater than the LG of Con. Overall, heterogeneity of muscles and between legs was evident in MFC_{DMD}, with at least one relatively preserved muscle in each functional compartment of the thigh. These relatively unaffected muscle(s) in each compartment likely contributed to the MFC_{DMD} remaining functional in her daily activities.

Strength and function of female carrier of DMD

The MFC_{DMD} participated in assessments of knee extension strength, functional ability (time to ascend 4 steps and 10 m walk/run), and the 6 minute walk test. Her knee extension strength was markedly lower than unaffected females of similar age when compared to literature values (Table 2) [37,38]. Overall, the deterioration in several muscle groups in her lower extremity likely contributed to reduced strength, as well as affected some aspects of her functional abilities during the testing. The subject demonstrated decreased functional ability (requiring the use of handrails to ascend stairs) and substantial gait deviations including a high steppage gait, bilateral foot drop (most notably on the left), genu recurvatum, and positive Trendelenburg indicative of hip weakness. The observation of foot drop being most pronounced for the left foot during gait and the clinical assessment with a prescription of an ankle foot orthosis for the left leg were consistent with greater involvement in the TA observed with the MR measures.

The 6 minute walk test has long been widely used in individuals with compromised cardiac and pulmonary function [39] and standardized guidelines have been established by the American Thoracic Society [40]. More recently the 6-minute walk test has been proposed as an outcome measure of various neuromuscular diseases, including Duchenne muscular dystrophy [41,42] and myotonic dystrophies [43]. In a large cohort of 173 healthy females between the age of 40 and 80 years, a regression equation was developed based on age, height, and body mass [44]. The subject of this case report walked 467 m for the 6 minute walk test, which was 25% below the predicted normative value of 619 m for unaffected adults. Her distance walked was similar to those with myotonic dystrophy type I that had a stage 3 or 4 rating on the Muscle Impairment Rating Scale [43], and well above average values of 5–12 year old boys with DMD (366±83 m) [42].

Summary and Conclusions

In summary, in this study we utilized MRI and MRS to quantify cross-sectional area, lipid infiltration, contractile area, and T_2 in lower extremity muscles in a MFC_{DMD}. These MR measures revealed considerable heterogeneity among muscles and between legs in the MFC_{DMD}, with progression of involvement observed in specific muscles over 21 months. The affected muscles observed using MR were associated with functional and strength deficits. Future studies would benefit from a larger cohort of female carriers with a range of clinical presentations. Overall, our results indicate that MRI/MRS may be a valuable non-invasive tool for identifying involved muscles and following progression of disease that could be targeted for therapeutic interventions in this population.

Acknowledgments

We thank Derek Wilson, Nicholas Israel-Stahre, and William Triplett for assistance with imaging analysis. This study was supported by the Wellstone Muscular Dystrophy Center (1U54RO52646-01A1) and NIH (RC1 AR058189). SCF was supported by an MDA development grant (175552) and AHA post-doctoral fellowship.

Abbreviations

AL	adductor longus
AM	adductor magnus
BFl	biceps femoris-long head
BFs	biceps femoris-short head
Con	control
CSA_{max}	maximal cross sectional area
CSI	chemical shift imaging
DMD	Duchenne muscular dystrophy
ED	end diastolic
EDL	extensor digitorum longus
EDV	end diastolic volume
ES	end systolic
ESV	end systolic volume
GE	gradient echo
Gra	gracilis
^1H	hydrogen
^1H_2O	water
LG	lateral gastrocnemius
m	meter
MIPAV	Medical Image Processing, Analysis and Visualization
MRI	magnetic resonance imaging
MRS	magnetic resonance spectroscopy
MG	medial gastrocnemius

Nm	newton meter
NNLS	non negative least squares
Per	peroneas longus and brevis
Rt	right
RF	rectus femoris
Sar	sartorius
SM	semimembranosus
Sol	soleus
SPIR	spectral presaturation by inversion recovery
ST	semitendinosis
T_1	spin lattice relaxation time
T_2	transverse relaxation time
TA	tibialis anterior
TE	echo time
TP	tibialis posterior
TR	repetition time
VI	vastus intermedius
VL	vastus lateralis
VM	vastus medialis

References

1. Hoffman EP, Brown RH, Kunkel LM. Dystrophin: the protein product of the Duchenne muscular dystrophy locus. Cell. 1987; 51:919–928. [PubMed: 3319190]
2. Bushby K, Finkel R, Birnkrant DJ, Case LE, Clemens PR, Cripe L, Kaul A, Kinnett K, McDonald C, Pandya S, Poysky J, Shapiro F, Tomezsko J, Constantin C. Diagnosis and management of Duchenne muscular dystrophy, part 1: diagnosis, and pharmacological and psychosocial management. The Lancet Neurology. 2010; 9:77–93.
3. Ceulemans BP, Storm K, Reyniers E Jr, Callewaert L, Martin JJ. Muscle Pain as the Only Presenting Symptom in a Girl With Dystrophinopathy. Pediatric Neurology. 2008; 38:64–66. [PubMed: 18054699]
4. Hoogerwaard E, Bakker E, Ippel P, Oosterwijk J, Majoor-Krakauer D, Leschot N, Van Essen A, Brunner H, van der Wouw P, Wilde A, de Visser M. Signs and symptoms of Duchenne muscular dystrophy and Becker muscular dystrophy among carriers in the Netherlands: a cohort study. The Lancet. 1999; 353:2116–2119.
5. Yilmaz A, Gdynia H-J, Ludolph AC, Klingel K, Kandolf R, Sechtem U. Cardiomyopathy in a Duchenne Muscular Dystrophy Carrier and Her Diseased Son: Similar Pattern Revealed by Cardiovascular MRI. Circulation. 2010; 121:239.
6. Walcher T, Kunze M, Steinbach P, Sperfeld A-D, Burgstahler C, Hombach V, Torzewski J. Cardiac involvement in a female carrier of Duchenne muscular dystrophy. International Journal of Cardiology. 2010; 138:302–305. [PubMed: 18706718]
7. Moser H, Emery A. The manifesting carrier in Duchenne muscular dystrophy. Clin Genet. 1974; 5:271–284. [PubMed: 4854942]

8. Song T-J, Lee K-A, Kang S-W, Cho H, Choi Y-C. Three Cases of Manifesting Female Carriers in Patients with Duchenne Muscular Dystrophy. Yonsei Med J. 2011; 52:192–195. [PubMed: 21155054]
9. Boyd Y, Buckle V, Holt S, Munro E, Hunter D, Craig I. Muscular dystrophy in girls with X;autosomal translocations. J Med Genet. 1986; 23:484–490. [PubMed: 3806636]
10. Gualandi F, Brioschi S, Falzarano MS, Bovolenta M, Armaroli A, Trabanelli C, Rimessi P, Merlini L, Mercuri E, Pane M, Bertini E, D'Amico A, Sicilano G, Tedeschi S, Pini A, De Grandis D, Mongini T, Ferlini A. Whole Genetic and protein characterization in DMD symptomatic female carriers excludes correlation with X-inactivation and transcriptional DMD allele balancing. Neuromuscular disorders. 2011; D21:517.
11. Arahata K, Ishihara T, Kamakura K, Tsukahara T, Ishiura S, Baba C, Matsumoto T, Nonaka I, Sugita H. Mosaic expression of dystrophin in symptomatic carriers of Duchenne's muscular dystrophy. N Engl J Med. 1989; 19:138–142. [PubMed: 2643040]
12. Griggs RC, Mendell JR, Brooke MH, Fenichel GM, Miller JP, Province M, Moxley RT, Huntzinger D, Vaughn A, Cohen M. Clinical investigation in Duchenne dystrophy: V. Use of creatine kinase and pyruvate kinase in carrier detection. Muscle Nerve. 1985; 8:60–67. [PubMed: 4058458]
13. Norman A, Harper P. A survey of manifesting carriers of Duchenne and Becker muscular dystrophy in Wales. Clin Genet. 1989; 36:31–37. [PubMed: 2766561]
14. Grain L, Cortina-Borja M, Forfar C, Hilton-Jones D, Hopkin J, Burch M. Cardiac abnormalities and skeletal muscle weakness in carriers of Duchenne and Becker muscular dystrophies and controls. Neuromuscular Disorders. 2001; 11:186–191. [PubMed: 11257476]
15. Meola G, Scarpini E, Silani V, Scarlato G. Manifesting carrier of X-linked Duchenne muscular dystrophy. Journal of the Neurological Sciences. 1981; 49:455–463. [PubMed: 7217994]
16. Yoon J, Kim SH, Ki C-S, Kwon M-J, Lim M-J, Kwon S-R, Joo K, Moon C-G, Park W. Carrier Woman of Duchenne Muscular Dystrophy Mimicking Inflammatory Myositis. J Korean Med Sci. 2011; 26:587–591. [PubMed: 21468271]
17. Matsumura K, Nakano I, Fukuda N, Ikehira H, Tateno Y, Aoki Y. Duchenne muscular dystrophy carriers. Proton spin-lattice relaxation times of skeletal muscles on magnetic resonance imaging. Neuroradiology. 1989; 31:373–376. [PubMed: 2594178]
18. Wang L, Salibi N, Wu Y, Schweitzer ME, Regatte RR. Relaxation times of skeletal muscle metabolites at 7T. Journal of Magnetic Resonance Imaging. 2009; 29:1457–1464. [PubMed: 19472422]
19. Gold GE, Han E, Stainsby J, Wright G, Brittain J, Beaulieu C. Musculoskeletal MRI at 3.0 T: Relaxation Times and Image Contrast. American Journal of Roentgenology. 2004; 183:343–351. [PubMed: 15269023]
20. Maier CF, Tan SG, Hariharan H, Potter HG. T2 quantitation of articular cartilage at 1.5 T. Journal of Magnetic Resonance Imaging. 2003; 17:358–364. [PubMed: 12594727]
21. Elliott MA, Walter GA, Swift A, Vandenborne K, Schotland JC, Leigh JS. Spectral quantitation by principal component analysis using complex singular value decomposition. Magnetic Resonance in Medicine. 1999; 41:450–455. [PubMed: 10204865]
22. Whittall KP, MacKay AL. Quantitative Interpretation of NMR Relaxation Data. J Magn Reson. 1989; 84:134–152.
23. Zhao Q, Patriotis P, Arias-Mendoza F, Stoyanova R, Brown TR. An interactive software for 3D chemical shift imaging data analysis and real time spectral localization and quantification. Proc Int Soc Mag Reson Med. 2005; 13:2465.
24. Mathur S, Lott DJ, Senesac C, Germain SA, Vohra RS, Sweeney HL, Walter GA, Vandenborne K. Age-Related Differences in Lower-Limb Muscle Cross-Sectional Area and Torque Production in Boys With Duchenne Muscular Dystrophy. Arch Phys Med Rehabil. 2010; 91:1051–1058. [PubMed: 20599043]
25. Brookes MH, Griggs RC, Mendell JR, Fenichel GM, Shumate JB, Pellegrino RJ. Clinical trials in Duchenne dystrophy. I: The design of the protocol. Muscle Nerve. 1981; 4:186–197. [PubMed: 7017401]

26. Glover GH, Schneider E. Three-point Dixon technique for true water/fat decomposition with B0 inhomogeneity correction. Magn Reson Med. 1991; 18:371–383. [PubMed: 2046518]
27. Wren TAL, Bluml S, Tseng-Ong L, Gilsanz V. Three-Point Technique of Fat Quantification of Muscle Tissue as a Marker of Disease Progression in Duchenne Muscular Dystrophy: Preliminary Study. Am. J. Roentgenol. 2008; 190:W8–W12. [PubMed: 18094282]
28. Gloor M, Fasler S, Fischmann A, Haas T, Bieri O, Heinimann K, Wetzel SG, Scheffler K, Fischer D. Quantification of fat infiltration in oculopharyngeal muscular dystrophy: Comparison of three MR imaging methods. Journal of Magnetic Resonance Imaging. 2011; 33:203–210. [PubMed: 21182140]
29. Kan HE, Scheenen TWJ, Wohlgemuth M, Klomp DWJ, van Loosbroek-Wagenmans I, Padberg GW, Heerschap A. Quantitative MR imaging of individual muscle involvement in facioscapulohumeral muscular dystrophy. Neuromuscular Disorders. 2009; 19:357–362. [PubMed: 19329315]
30. Loganathan R, Bilgen M, Al-Hafez B, Smirnova IR. Characterization of alterations in diabetic myocardial tissue using high resolution MRI. Int J Cardiovasc Imaging. 2005; 22:81–90. [PubMed: 16362172]
31. Foley JM, Yayaraman RC, Prior BM, Pivarnik JM, Meyer RA. MR measurements of muscle damage and adaptation after eccentric exercise. Journal of Applied Physiology. 1999; 87:2311–2318. [PubMed: 10601183]
32. Mathur S, Vohra RS, Germain SA, Forbes S, Bryant ND, Vandenborne K, Walter GA. Changes in muscle T2 and tissue damage after downhill running in mdx Mice. Muscle &Nerve. 2011; 43:878–886. [PubMed: 21488051]
33. Marqueste T, Giannesini B, Fur YL, Cozzone PJ, Bendahan D. Comparative MRI analysis of $_{T2}$ changes associated with single and repeated bouts of downhill running leading to eccentric-induced muscle damage. J Appl Physiol. 2008; 105:299–307. [PubMed: 18450983]
34. Ploutz-Snyder LL, Nyren S, Cooper TG, Potchen EJ, Meyer RA. Different effects of exercise and edema on T_2 relaxation in skeletal muscle. Magn Reson Med. 1997; 37:676–682. [PubMed: 9126941]
35. Marden FA, Connolly AM, Siegel MJ, Rubin DA. Compositional analysis of muscle in boys with Duchenne muscular dystrophy using MR imaging. Skeletal Radiol. 2005; 34:140–148. [PubMed: 15538561]
36. Akima H, Lott D, Senesac C, Deol J, Germain S, Arpan I, Bendixen R, Lee Sweeney H, Walter G, Vandenborne K. Relationships of thigh muscle contractile and non-contractile tissue with function, strength, and age in boys with Duchenne muscular dystrophy. Neuromuscular Disorders. 2012 Jan; 22(1):16–25. [PubMed: 21807516]
37. Greeves JP, Cable NT, Reilly T, Kingsland C. Changes in muscle strength in women following the menopause: a longitudinal assessment of the efficacy of hormone replacement therapy. Clin. Sci. 1999; 97:79–84. [PubMed: 10369797]
38. Ditroilo M, Forte R, Benelli P, Gambarara D, De vito G. Effects of age and limb dominance on upper and lower limb muscle function in healthy males and females aged 40–80 years. Journal of Sports Sciences. 2010; 28:667–677. [PubMed: 20397097]
39. Guyatt GH, Sullivan MJ, Thompson PJ, Fallen EL, Pugsley SO, Taylor DW, LB B. The 6-minute walk: a new measure of exercise capacity in patients with chronic heart failure. Can Med Assoc J. 1985; 132:919–923. [PubMed: 3978515]
40. Society AT. ATS Statement: Guidelines for the Six-Minute Walk Test. Am. J. Respir. Crit. Care Med. 2002; 166:111–117. [PubMed: 12091180]
41. McDonald CM, Henricson EK, Han JJ, Abresch RT, Nicorici A, Atkinson L, Elfring GL, Reha A, Miller LL. The 6-minute walk test in Duchenne/Becker muscular dystrophy: Longitudinal observations. Muscle &Nerve. 2010; 42:966–974. [PubMed: 21038378]
42. McDonald CM, Henricson EK, Han JJ, Abresch RT, Nicorici A, Elfring GL, Atkinson L, Reha A, Hirawat S, Miller LL. The 6-minute walk test as a new outcome measure in Duchenne muscular dystrophy. Muscle &Nerve. 2010; 41:500–510. [PubMed: 19941337]
43. Kierkegaard M, Tollbäck A. Reliability and feasibility of the six minute walk test in subjects with myotonic dystrophy. Neuromuscular Disorders. 2007; 17:943–949. [PubMed: 17869516]

44. Enright PL, Sherrill DL. Reference Equations for the Six-Minute Walk in Healthy Adults. Am J. Respir. Crit. Care Med. 1998; 158:1384–1387. [PubMed: 9817683]

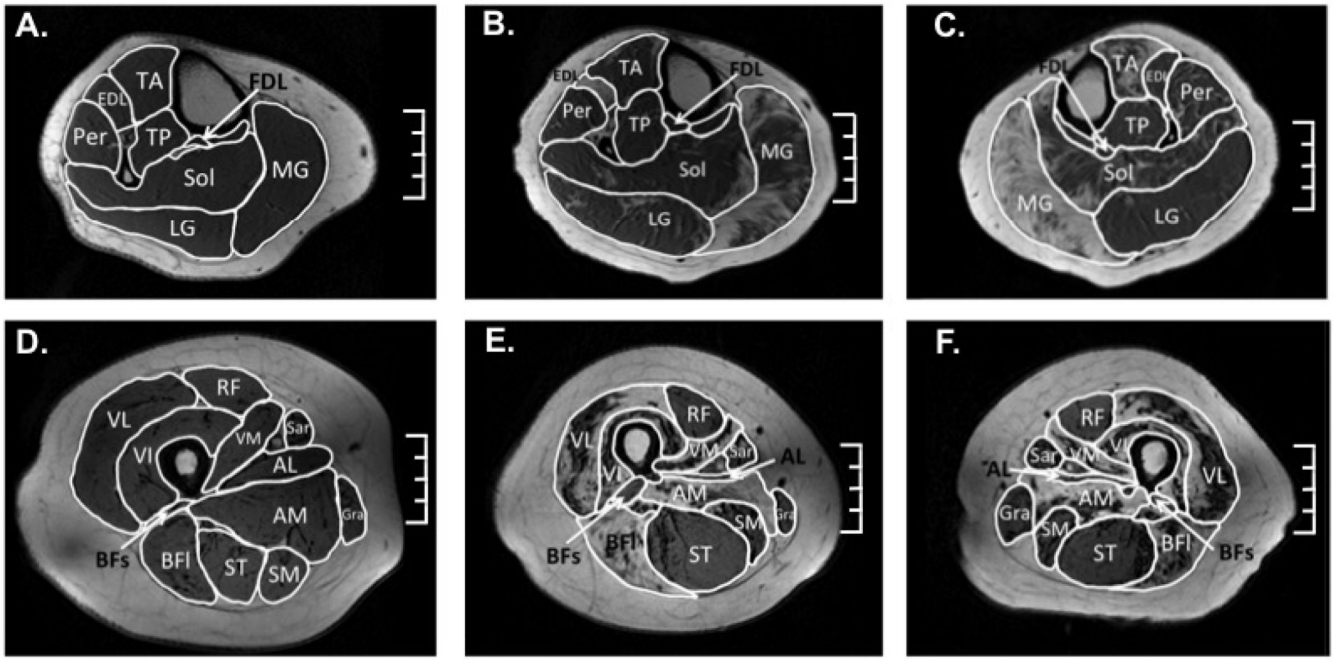

Figure 1.

Example axial T_1-weighted gradient echo images used for cross sectional area analysis of the right lower leg in a control subject (A) and of the right (B) and left (C) leg of the MFC_{DMD}. Representative axial thigh image of a control (D) and the right (E) and left (F) thigh of the MFC_{DMD}. Scale = 4 cm. used for CA analysis.

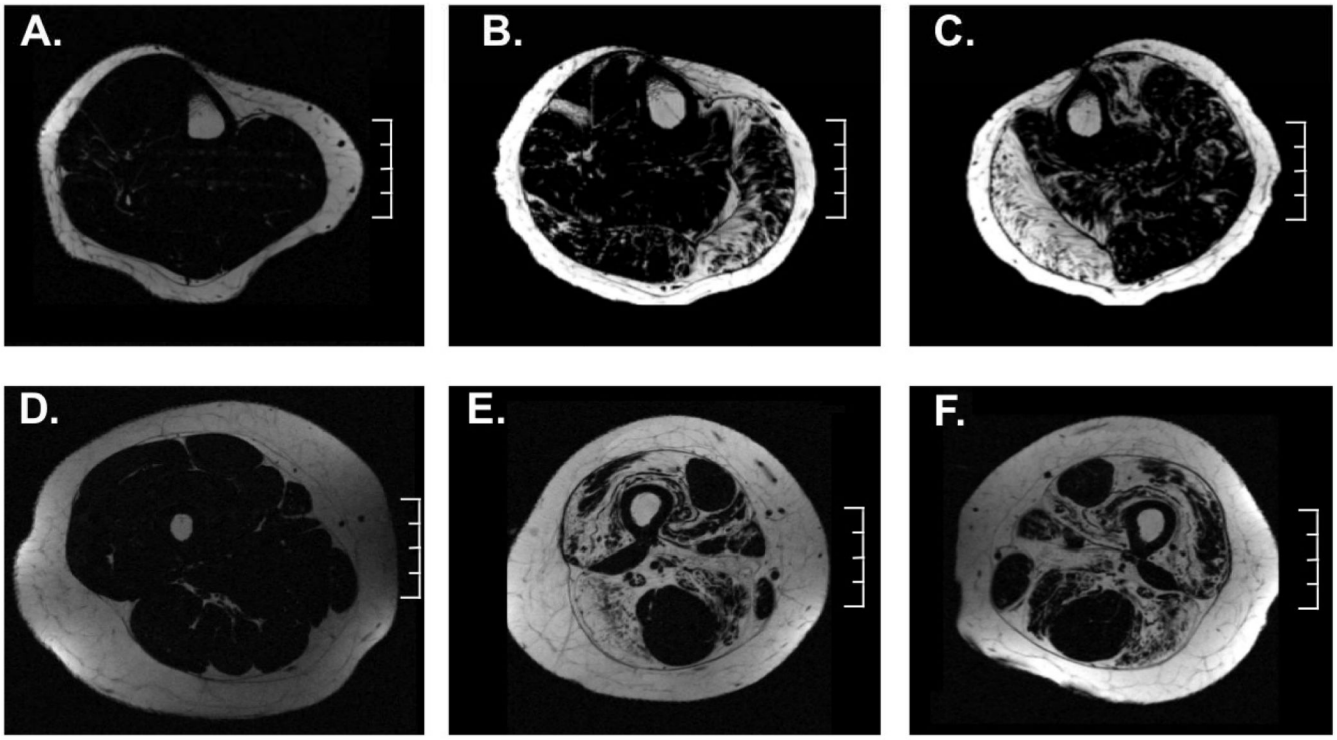

Figure 2.
Representative axial 3-pt Dixon lipid maps of the right lower leg in a control subject (A) and of the right (B) and left (C) lower leg of the MFC_{DMD}. Representative axial thigh lipid map of a control subject (D) and the right (E) and left (F) thigh of the MFC_{DMD}. Scale = 4 cm.

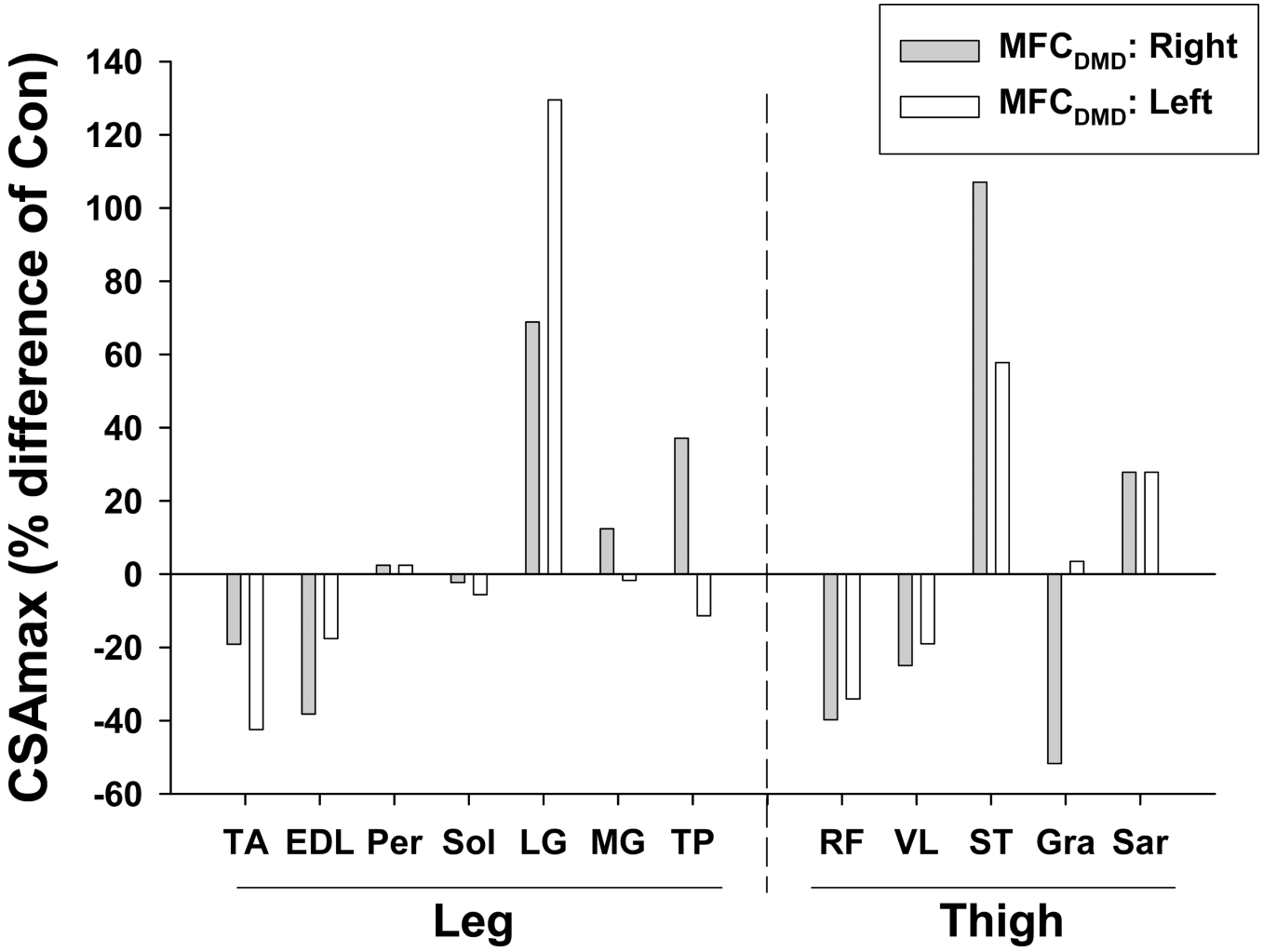

Figure 3.
Maximum cross-sectional area (CSA_{max}) in the right and left lower extremity of the MFC_{DMD} expressed relative to an unaffected control subject (Con) of similar age and body mass.

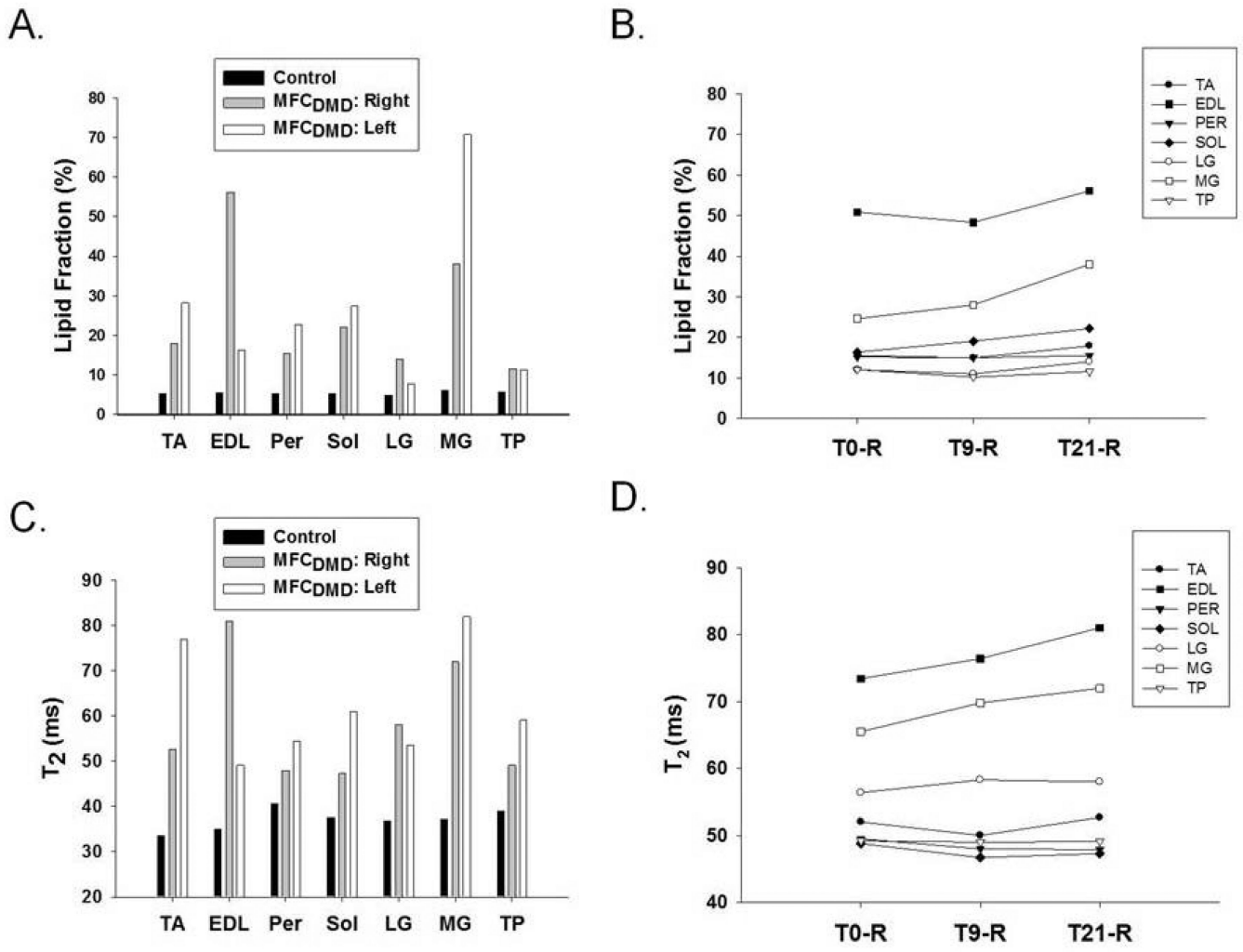

Figure 4.

Lipid fraction of leg muscles in a control subject and in the left and right lower leg of the MFC_{DMD} (A) and longitudinal changes at three time points at baseline (T0-R), 9 months (T9-R), and 21 months (T21-R) of the right leg in the MFC_{DMD} (B). T_2 measures in a control subject and in the left and right leg of the MFC_{DMD} (C) and longitudinal changes at three time points of the right lower leg in the MFC_{DMD} (D).

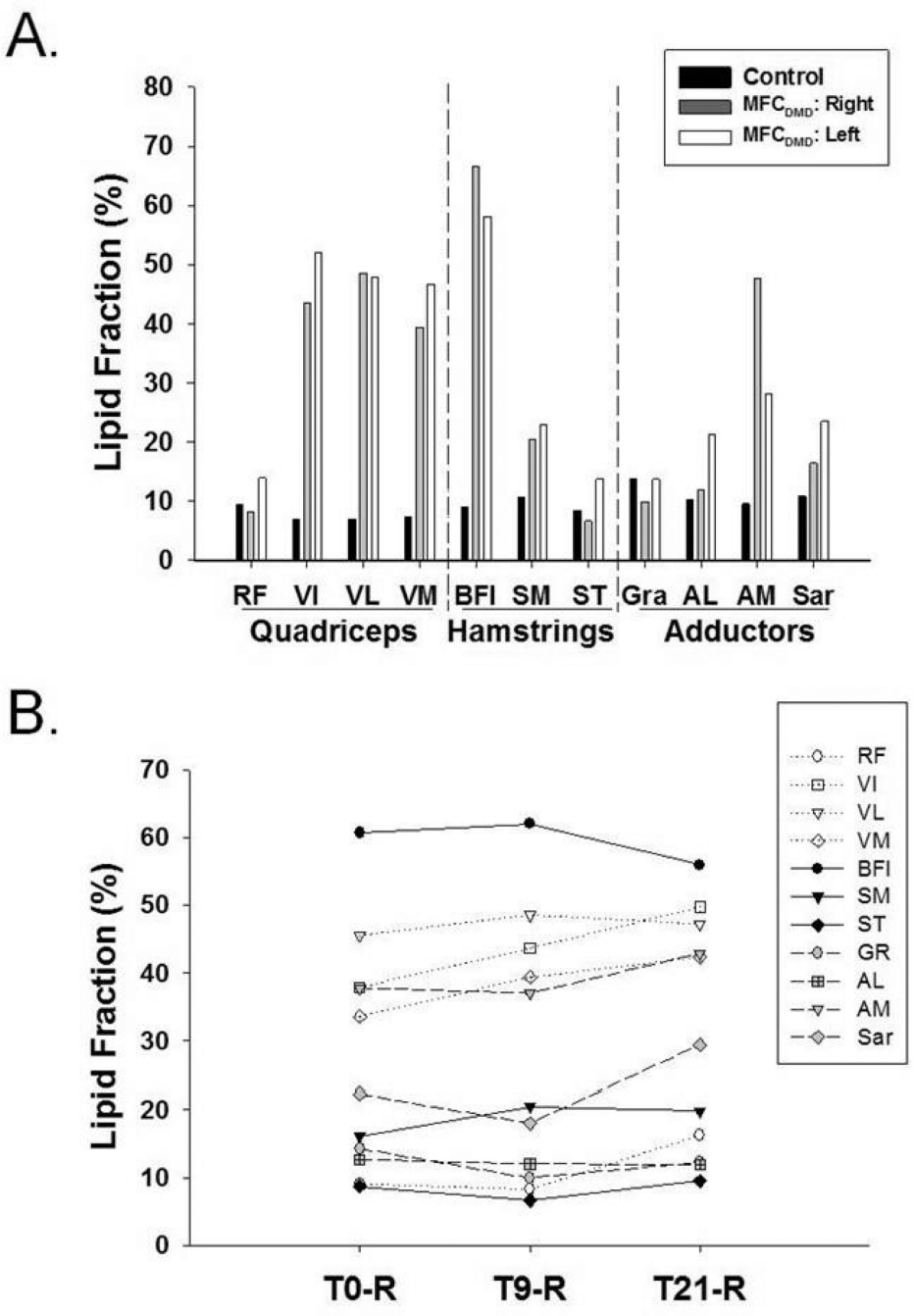

Figure 5.

Lipid fraction of quadriceps, hamstring, and adductor muscles in the control and right and left thigh of the MFC_{DMD} (A) and longitudinal changes at three time points at baseline (T0-R), 9 months (T9-R), and 21 months (T21-R) of thigh muscles in the MFC_{DMD} (B).

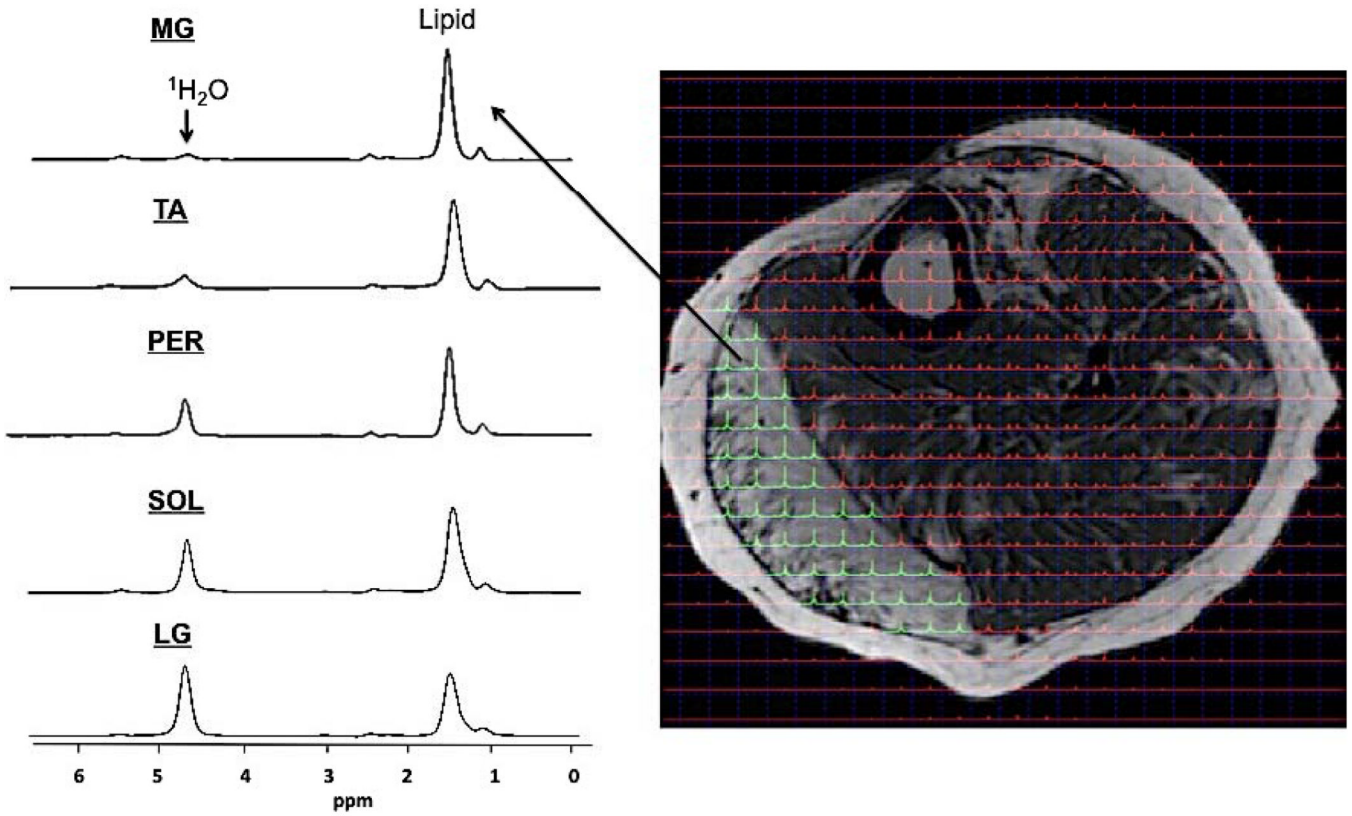

Figure 6.

Spectrum obtained from left lower leg muscles of the MFC_{DMD} using 2D PRESS CSI. Spectra were obtained using a 12×12 matrix (1×1 cm voxels), zero filled to 24×24, and overlaid on an axial image. Spectra were summed within each muscle to create a single spectrum and relative lipid fraction measures were calculated for the MG, Per, TA, Sol, and LG. These values showed considerable heterogeneity among muscles (MG: 0.93; TA: 0.84; Per: 0.72; Sol: 0.68; LG: 0.55) and were greater than average Con values (0.23).

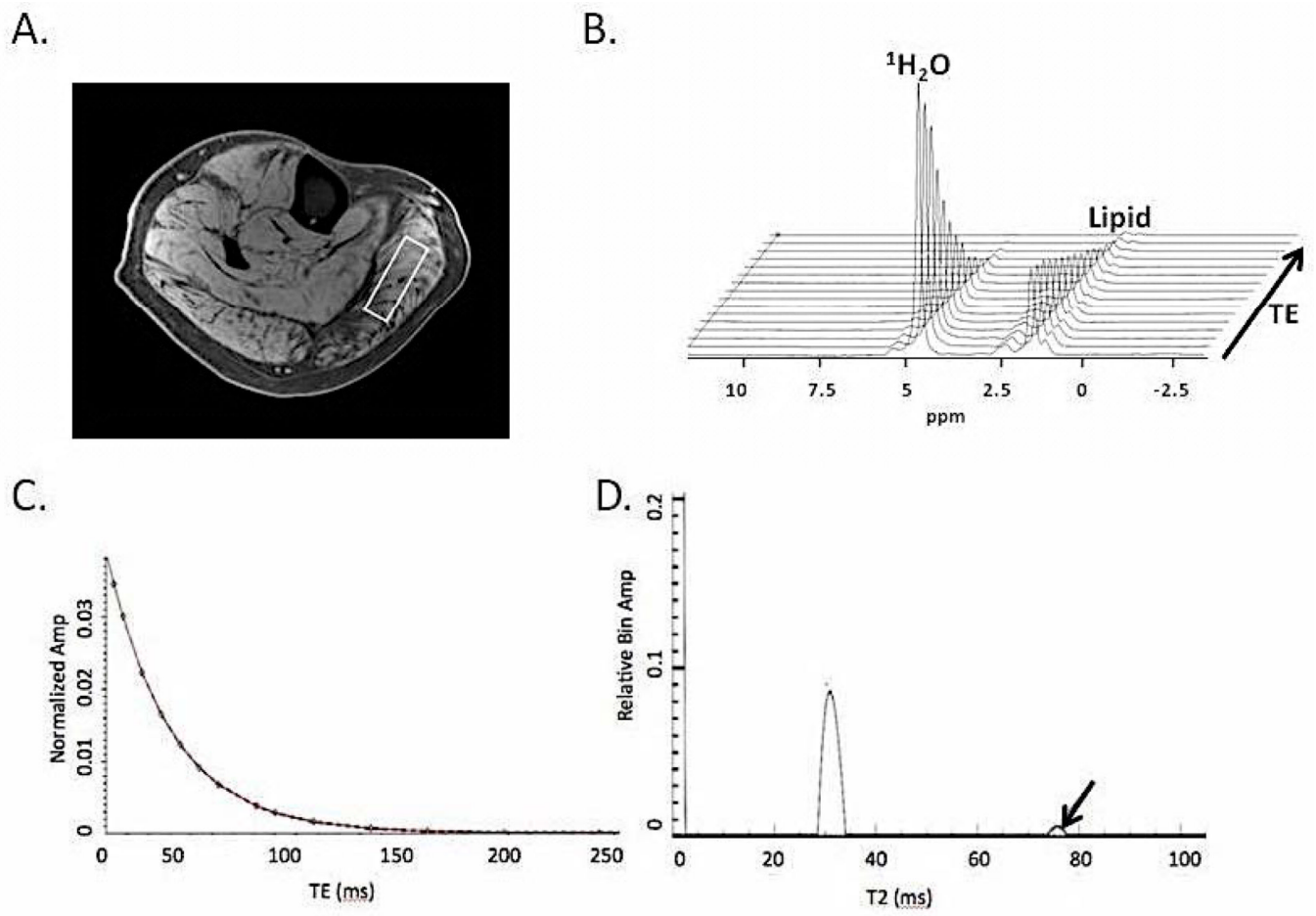

Figure 7.

Spectroscopic relaxometry of the right medial gastrocnemius (MG) of the MFC_{DMD} using single voxel STEAM (A) was acquired at 16 logarithmically spaced echoes (B). T_2 of ^1H_2O was determined using a mono-exponential model (C). T_2 was greater in the MG (32.4 ms) than in an unaffected Con (28.5 ms). Furthermore, non-negative least square analysis revealed a long T_2 component (arrow) in the MFC_{DMD}, suggesting edema-like fluid accumulation (D).

Table 1

Maximum cross sectional area (CSA_{max}) of lower leg and thigh muscles in the control subject (Con) and a manifesting female carrier of DMD (MFC_{DMD}) at three time points: TO-R, baseline, right lower extremity; T9-R, 9 months, right lower extremity; T21-R, 21 months, right lower extremity; T21-L, 21 months, left lower extremity. Data shown in bold have a >20% difference than Con. Data shown in italics represents the left side being >20% different from the right at T21.

		CSA_{max} (cm^2)				
		Con	MFC_{DMD}			
			T0-R	T9-R	T21-R	T21-L
Lower Leg	**TA**	7.3	6.3	6.1	5.9	***4.2***
	EDL	3.4	2.9	2.8	**2.1**	*2.8*
	Per	4.1	4.4	4.4	4.2	4.2
	Sol	21.4	23.5	21.4	20.9	20.2
	LG	6.1	**10.0**	**9.9**	**10.3**	***14.0***
	MG	11.3	**13.7**	12.5	12.7	11.1
	TP	3.5	**4.3**	4.1	**4.8**	*3.1*
Thigh	**RF**	8.8	**5.4**	NA	**5.3**	**5.8**
	VL	16.8	13.8	**13.2**	**12.6**	13.6
	ST	7.1	**14.1**	NA	**14.7**	***11.2***
	Gra	2.9	**1.8**	**1.3**	**1.4**	*3.0*
	Sar	1.8	**2.2**	**2.4**	**2.3**	**2.3**

CSA_{max} for RF and ST at the second time point (T9-R) were not within the FOV of images, and therefore these values were not available (NA).

Table 2

Strength and functional measures acquired on the MFC_{DMD}

Strength/Function	Score	Normative Data
Knee Extensor Peak Torque (Nm)	**22.4 (R), 27.1 (L)**	132±31[a]; 115±9[b]
10 m walk/run (s)	6.34	NA
Stair Climb, 4 steps (s)	2.75	NA
6 min walk test (m)	**487**	619±78[c]
Modified Brooke Lower Extremity Scale	**2**	1

Literature values for strength and function measures were obtained from a[38], b[37], and c[44]. Values in bold indicate that the MFC_{DMD} appears to be outside the normal range for unaffected individuals of similar age and same gender. NA indicates that normative values for similar age and gender were not available for the protocol implemented in MFC_{DMD}.